Conformational Features of 5′-*O*-[*N*-(L-Alanyl)sulfamoyl]adenosine, a Substrate Analogue of Alanyl-tRNA Synthetase, Studied by ^{1}H-NMR and Energy Calculation Methods

Toshimasa ISHIDA,*[a] Yasuko IN,[a] Yuki HIRASE,[a] Kouji SHIHODA,[a] Masatoshi INOUE,[a] Miyoko KAMIGAUCHI,*[b] Makiko SUGIURA[b] and Narao TAKAO[b]

Osaka University of Pharmaceutical Sciences,[a] 2–10–65 Kawai, Matsubara, Osaka 580, Japan and Kobe Women's College of Pharmacy,[b] 4–19–1 Motoyamakita-machi, Higashinada-ku, Kobe 658, Japan. Received October 5, 1992

The solution conformation of 5′-*O*-[*N*-(L-alanyl)sulfamoyl]adenosine (ala-SA), an analogue of alanyl-AMP, was studied by ^{1}H-NMR spectroscopic and energy calculation methods for elucidating the substrate-specificity of the cognate alanyl-tRNA synthetase. The ala-SA molecule existed in several conformational equilibria such as *anti*⇌*syn*, C3′-*endo*⇌C2′-*endo* and *gauche*·*gauche*⇌*gauche*·*trans* (or *trans*·*gauche*) orientations concerning the glycosyl bond, ribose puckering and exocyclic C4′–C5′ bond, respectively. However, their populations were solvent-dependent, and the major form in D_2O solution could be characterized as the *anti*-C2′-*endo*-*gauche*·*gauche* conformation, although no predominant conformation, except for C2′-*endo* ribose puckering, existed in dimethyl sulfoxide solution. Possible conformers satisfying the NMR data were surveyed using empirical energy calculations, and the solution conformation of the ala-SA molecule was compared with its crystal conformation.

Keywords 5′-*O*-[*N*-(L-alanyl)sulfamoyl]adenosine; alanyl-AMP analogue; molecular conformation; ^{1}H-NMR analysis; energy calculation

Aminoacyl-tRNA synthetase (ARS) catalyses the esterification of a particular tRNA with its corresponding amino acid (aa), the first step for protein biosynthesis, according to a proposed mechanism[1]:

$$\text{aa} + \text{ARS} + \text{ATP} \rightleftharpoons \text{aa-AMP}\cdot\text{ARS} + \text{PPi}$$

$$\text{aa-AMP}\cdot\text{ARS} + \text{tRNA} \rightleftharpoons \text{aa-tRNA} + \text{ARS} + \text{AMP}$$

In order to produce the biologically active protein, exact recognition of the aminoacyl-AMP (aa-AMP) by the cognate ARS is required. Recent protein crystallography revealed the three-dimensional structures of tyrosyl-,[2,3] methionyl-,[4,5] glutamyl-[6] and aspartyl-ARS[7] and provided information concerning the nature of the binding with the cognate aa-AMP and/or tRNA molecules. Concerning the question of how the enzyme discriminates between the cognate and noncognate aa-AMPs, however, no clear answer has yet been provided because of the limited X-ray data and their resolution. As a possible step towards answering this question, it would be profitable to analyse the most favorable conformations of a series of aa-AMPs and to characterize respective conformational features.

The studies of aa-AMP molecular conformations have been rather limited[8~11] because of the high lability of the ester linkage between the AMP and amino acid moieties. Recently, 5′-*O*-[*N*-(L-alanyl)sulfamoyl]adenosine (ala-SA, **1**) was shown to be a chemically stable compound which, as well as the cognate alanyl-AMP (**2**), can be selectively recognized by ala-ARS.[12] Ala-SA has a sulfamoylamide linkage instead of the phosphoester linkage of ala-AMP, but the bond lengths and angles are very similar.[12] To investigate the conformational features of ala-SA, this paper deals with its conformation in solution studied by ^{1}H-NMR and empirical energy calculation methods and compares this with the solid state conformation.[12] The chemical structures of **1** and **2** are shown in Fig. 1.

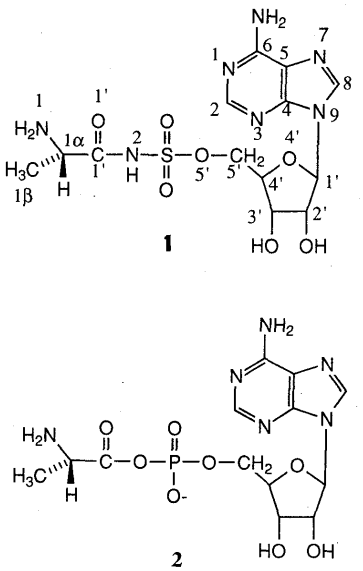

1 **2**

Fig. 1. Chemical Structures of Ala-SA (**1**) and Alanyl-AMP (**2**)
The atomic numbering used is given in **1**.

Experimental

Materials Ala-SA was synthesized as described in a previous paper.[12] The purity was checked by the HPLC elution profile and ^{1}H-NMR measurements. All other materials were commercial preparations (reagent grade) and were used without further purification.

^{1}H-NMR Measurement ^{1}H-NMR measurements were carried out on a Varian VXR-500 NMR spectrometer at 294 K—295 K. Sample concentrations were gravimetrically adjusted to 5 mg/0.5 ml (*ca.* 0.024 M). The D_2O and DMSO-d_6 (dimethyl sulfoxide-d_6) were used as solvent. Respective sample solutions were degassed 4 times using the freeze-pumpthaw technique and then sealed under vacuum. The deuterium resonance of the solvent D_2O or DMSO-d_6 was used as the lock signal, and the chemical shifts were measured with respect to an internal reference of DSS (2,2-dimethyl-2-silapentane-5-sulfonate) for D_2O or TMS (tetramethylsilane) for DMSO. Signal assignments and coupling constants were performed by spin multiplicity, standard successive decoupling and two-dimensional correlated spectroscopy (COSY). The chemical shifts and corresponding coupling constants of the complicated H2′–H5′ and H5″ protons were obtained from a computer fit of the spectra using the Varian LAME (LAOCON) program. The steady-state nuclear Overhauser effect

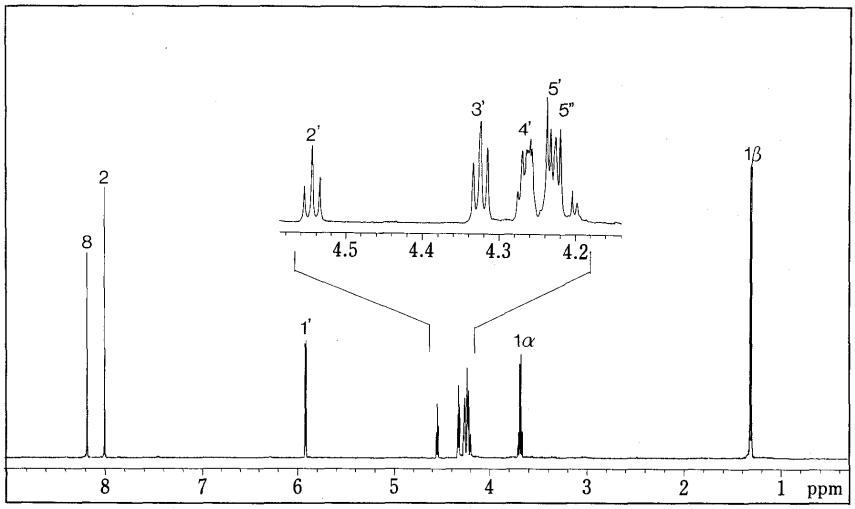

Fig. 2. Peak Assignment of 500-MHz ^{1}H-NMR Spectrum of Ala-SA in D_2O Solution

(NOE) was estimated from the difference between the on- and off-resonance spectra. Saturation power levels were chosen by measuring the minimum power necessary to completely suppress a given multiplet. The proton spin-lattice relaxation time (T_1) measurements were carried out by the inversion recovery (180°-τ-90°-t) method. The NOEs and T_1 were measured two to three times and the mean calculated.

Conformational Energy Calculation The energies for various conformers were calculated by the molecular mechanics method. The energy functions included in the calculation were non-bonded (E_{nb}), electrostatic (E_{elec}) and torsional (E_{tot}) energies:

$$E_{nb}=\sum_{i>j}\sum(-A_{ij}r_{ij}^{-6}+B_{ij}r_{ij}^{-12}) \quad (1)$$

$$E_{elec}=\sum_{i>j}\sum 332.0\cdot Q_i\cdot Q_j\cdot r_{ij}\cdot\varepsilon^{-1} \quad (2)$$

$$E_{tot}=\sum_{k=1}^{N} 1/2\cdot V_k\cdot(1\times\cos X\theta_k) \quad (3)$$

In Eqs. 1 and 2, r_{ij} is the distance between atom i and j in Å; A_{ij} and B_{ij} are the coefficients in the Lennard-Jones '6—12' potential function; Q_i is the Coulombic net charge on atom i, calculated by the CNDO/2 method; ε is the dielectric constant and was taken as 4.0, close to the experimental value for biomolecules in polar media[13]; V_k in Eq. 3 is the barrier potential for the internal rotation about the k-th torsion angle (θ_k); X is the periodicity of the barrier; N is the number of variable torsion angles. Calculations of Eqs. 1 and 3 were performed with the supplied data set,[14] where the torsional parameters of P–O and P–N bonds were used for those of S–O and S–N bonds, respectively. For energy minimization, each torsion angle as a variable parameter was optimized by the Powell algorithm.[15]

Results

Proton Assignment and Coupling Constant Determination The assignment of the proton signals was determined using the standard decoupling and COSY techniques, and the ^{1}H-NMR spectrum in D_2O is given in Fig. 2. The chemical shifts and coupling constants in D_2O and DMSO-d_6 solutions are summarized in Table I, where the estimated standard deviations are 0.001 ppm for the chemical shift and *ca.* 0.5 Hz for the coupling constant. The chemical shifts for protons H2′—H5′,H5″ and the corresponding coupling constants were obtained from the spin simulation. The best-fitting computer simulation for protons H3′—H5′,H5″ in D_2O is given in Fig. 3. No significant concentration-dependence (0.02—0.1 M) was observed for the chemical shifts, and this suggests that the data in Table I were obtained under conditions free from significant intermolecular association. Table I indicates that the chemical shifts and coupling constants of ala-SA are solvent-

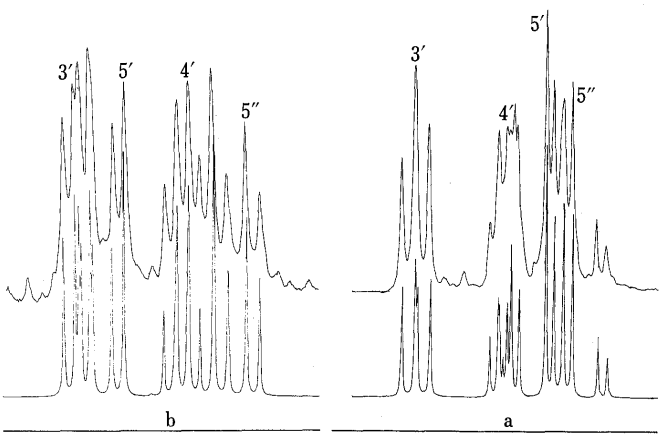

Fig. 3. Spectra of Ala-SA H3′–H5′,H5″ Proton Regions (Upper) and Their Computer Simulations (Lower) in D_2O (a) and DMSO (b) Solutions

TABLE I. Proton Chemical Shifts (δ, ppm), Coupling Constants (J, Hz) and Spin-Lattice Relaxation Time (s) in D_2O and DMSO-d_6 Solutions at 21°C

	D_2O	DMSO-d_6
Chemical shift		
H8	8.182 (s)[a]	8.370 (s)
H2	8.003 (s)	8.131 (s)
H6(NH_2)		7.274 (s)
H1′	5.917 (d)	5.900 (d)
H2′	4.545 (m)	4.593 (m)
H3′	4.325 (m)	4.152 (m)
H4′	4.266 (m)	4.086 (m)
H5′	4.243 (m)	4.134 (m)
H5″	4.216 (m)	4.053 (m)
H1α	3.686 (q)	3.473 (q)
H1β(CH_3)	1.312 (d)	1.292 (d)
Coupling constant		
$J_{1'2'}$	5.0	5.5
$J_{2'3'}$	5.1	4.9
$J_{3'4'}$	4.4	3.6
$J_{4'5'}$	2.4	3.6
$J_{4'5''}$	3.4	4.2
$J_{5'5''}$	−11.6	−10.1
$J_{1\alpha1\beta}$	7.0	7.0
Spin-lattice relaxation time (T_1)		
$(T_1)_8$	2.3	2.2
$(T_1)_{1'}$	3.7	2.1

a) The letters s, d, m and q in parentheses imply proton multiplicity of singlet, doublet, multiplet and quartet, respectively.

dependent to some extent, implying different conformations in the two solvents.

Conformational Analysis by ^{1}H-NMR Data A) Glycosyl Bond In nucleosides and nucleotides, stable conformations about the glycosyl bond are found in both the *anti* and *syn* forms; the torsion angle of C4–N9–C1′–O4′ is usually in the range of 180—250° (= −110°) for the *anti* and 30—90° for the *syn* conformation. Measurements of T_1 values for H8 and H1′ protons have been demonstrated to be useful for the estimation of possible *anti*/*syn* population.[16-18] Assuming that the ratio $(T_1)_8/(T_1)_{1'}$ is 0.53 for the *anti* and 1.52 for the *syn* conformation,[17] the conformation could be roughly estimated by the following equation:

$$(T_1)_8/(T_1)_{1'\text{obs}} = 0.53 \cdot P_{anti} + 1.52 \cdot P_{syn}$$

$$P_{anti} + P_{syn} = 1$$

where $(T_1)_8/(T_1)_{1'\text{obs}}$ represents the ratio of the observed T_1 values of H8 and H1′ protons, and P_{anti} and P_{syn} are the populations (%) of *anti* and *syn* conformers.

On the other hand, the conformer population about the glycosyl bond could also be semiquantitatively estimated from the chemical shift of the H2′ proton[19,20] using the equation:

$$\delta_{\text{obs}} = P_{syn} \cdot \delta_{syn} + P_{anti} \cdot \delta_{anti}$$

where 5.02 and 4.22 ppm for DMSO-d_6 and 5.24 and 4.40 ppm for D_2O solution were used as the δ values of *syn* and *anti*, respectively.[19]

B) Ribose Puckering The puckering population of the ribose ring has been assessed by assuming the equilibrium between the major C2′-*endo* and C3′-*endo* puckerings as follows[21].

$$\text{C3′-}endo\,(\%) = 100 \times [J_{3'4'}/(J_{1'2'} + J_{3'4'})]$$

C) Exocyclic C4′–C5′ Bond The conformation about the exocyclic C4′–C5′ bond has been discussed in terms of a blend of the *gauche*·*gauche* (*gg*), *gauche*·*trans* (*gt*) and *trans*·*gauche* (*tg*) according to the torsion angle (γ) of C3′–C4′–C5′–O5′; the value of γ is usually observed in the range of 36—70° for *gg*, 160—190° (= −170°) for *gt* and

TABLE II. Calculated Population (%) of Certain Conformations for the Ala-SA Molecule, Together with the Conformation Observed in the Crystalline State as a Comparison

		D_2O	DMSO-d_6	X-Ray
Glycosyl bond				
from $\delta_{H2'}$	*anti*	83.0	53.0	*anti*
	syn	17.0	47.0	
from T_1	*anti*	91.0	46.0	
	syn	9.0	54.0	
Ribose puckering	C3′-*endo*	42.0	39.0	C3′-*endo*
	C2′-*endo*	58.0	61.0	
C4′–C5′ bond	*gg*	72.0	52.0	*gt*
	tg or *gt*	28.0	48.0	

TABLE III. Selective NOE Enhancements (%) of Ala-SA in D_2O and DMSO-d_6 at 21 °C

Solvent	Irradiated	NOE observed at atom	
D_2O	H1α	CH_3	7.0
	CH_3	H	12.8
	H2′	H1′	5—6[a]
		H8	5—6[a]
DMSO-d_6	CH_3	H1α	10.9
	H2′	H1′	9.1
		H8	10.0
	H8	H1′	7.1
		H3′	5.9
	H6(NH_2)	H2	2.0

a) The values are not exact because of the overlapping of the H2′ proton with those of water.

TABLE IV. Energetically Refined Torsion Angles (°) of 10 Stable Conformers with C2′-*endo* and C3′-Ribose Puckerings, Together with Their Energies (kcal/mol) and Conformational Notations Concerning Adenosine Moiety

No.	χ	γ	β	α	ζ	ϕ	E	Notation
C2′-*endo* ribose puckering								
1	162.5	64.4	185.0	187.8	−86.0	170.0	−26.031	*anti-gg*
2	10.6	57.8	174.3	−159.0	−82.5	187.7	−25.995	*syn-gg*
3	183.6	53.7	171.0	−161.9	94.5	−174.2	−25.467	*anti-gg*
4	176.7	172.0	−168.7	52.0	−89.2	−173.7	−24.780	*anti-gt*
5	10.1	53.9	171.9	−137.7	−152.6	−175.4	−24.688	*syn-gg*
6	−0.3	167.2	−174.3	67.9	−83.4	−175.6	−24.662	*syn-gt*
7	−175.5	67.7	168.2	−160.8	150.1	175.4	−24.605	*anti-gg*
8	−171.4	55.4	170.7	−100.9	88.8	172.8	−24.578	*anti-gg*
9	−168.0	57.1	174.6	−80.7	−149.8	175.5	−24.345	*anti-gg*
10	−160.0	55.6	−178.8	−79.3	−90.8	176.5	−24.221	*anti-gg*
C3′-*endo* ribose puckering								
1	23.7	−62.8	158.6	−65.4	−81.4	177.7	−22.901	*syn-tg*
2	32.1	−64.7	167.9	5.0	−92.0	179.4	−22.790	*syn-tg*
3	13.3	43.1	−176.2	−173.3	−77.0	169.6	−21.930	*syn-gg*
4	31.1	−52.3	150.1	−78.3	153.1	178.1	−21.618	*syn-tg*
5	42.5	71.5	160.9	175.2	83.9	165.1	−21.422	*syn-gg*
6	−172.5	54.6	154.1	−91.6	−85.1	177.4	−21.414	*anti-gg*
7	39.9	−63.9	−178.5	−57.4	87.2	174.3	−21.323	*syn-tg*
8	−160.5	−52.8	155.3	−61.9	−80.1	178.5	−21.176	*anti-tg*
9	12.9	42.0	−178.4	−167.4	147.5	175.8	−21.150	*syn-gg*
10	31.0	180.0	167.4	28.8	−89.4	178.8	−20.878	*syn-gt*
Crystal-I	−167.0	−174.0	165.0	−68.9	170.0	171.0	−19.067	*anti-gt*
Crystal-II	−155.0	−170.2	−168.6	−72.0	−178.3	155.0	−18.554	*anti-gt*

-70——$-90°$ for *tg*. The following equation has been frequently used to estimate the contribution from the *gg* conformer[22]:

$$P_{gg}(\%) = 10 \times [13 - (J_{4'5'} + J_{4'5''})]$$

The conformational populations (%) about the glycosyl bond, ribose puckering and exocyclic C4′–C5-bond, estimated by the above-mentioned equations, are summarized in Table II, in which the conformation observed in the crystal is also given for comparison.

D) NOE Measurement The NOE measurement is a useful method for estimating conformational features, because it provides information concerning the proton–proton distance. The results measured for ala-SA in D_2O and DMSO-d_6 are given in Table III.

Conformational Analysis by Energy Calculation Possible conformational ranges for the adenosine moiety, though not definitive, were estimated by ^{1}H-NMR measurements. To define the complete conformation of the ala-SA molecule, however, the orientation around the sulfamoyl linkage connecting the adenosine and alanyl moieties must be known; thus it was examined by empirical energy calculations to search the energetically stable conformers.

As possible starting conformers, the following torsion angles were selected based on the NMR conformational analyses, a study of space-filling models and the general conformational characteristics of the 5′-substituted nucleotides, *i.e.*, $-150°$ or $30°$ for χ (C4–N9–C1′–O4′), C2′-*endo* or C3′-*endo* for ribose puckering, $\pm 60°$ or $180°$ for γ (C3′–C4′–C5′–O5′), $180°$ for β (C4′–C5′–O5′–S), $\pm 60°$ or $180°$ for α (C5′–O5′–S–N2), $\pm 90°$ or $180°$ for ζ (O5′–S–N2–C1′), and $-90°$ or $150°$ for φ (N1–C1α–C1′–N2). The torsion angle of the amide bond was taken as $180°$. All possible conformers having different starting torsion angles were energy-minimized. Among energy minimizations of different sets with ribose puckering of either the C2′-*endo* or C3′-*endo* form, the 10 most energetically-stable conformers for respective ribose puckerings are summarized in Table IV, together with the molecular conformations observed in the crystal structure (crystal-I and -II). The most stable conformers belonging to the C2′-*endo* and C3′-*endo* ribose puckerings, together with the conformation of crystal-I, are also shown in Fig. 4.

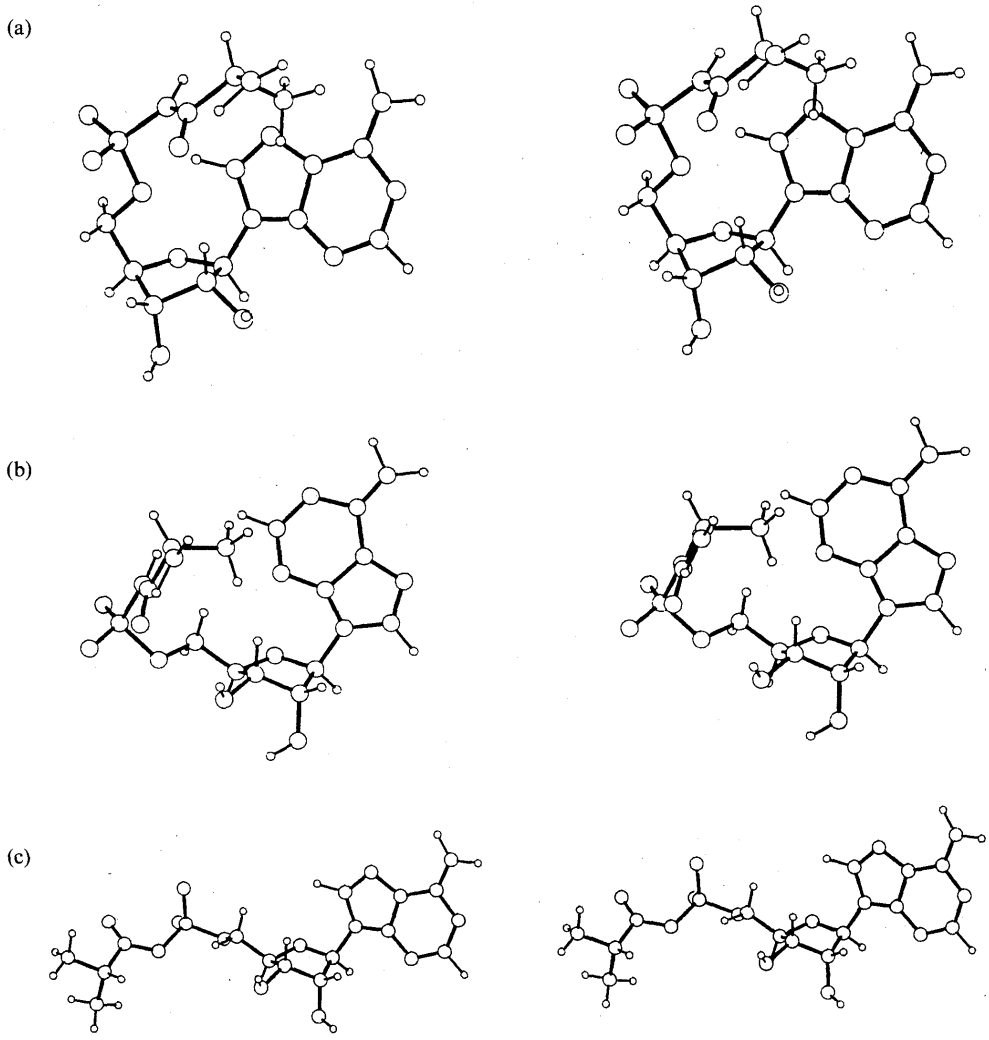

Fig. 4. Most Energetically-Stable Conformers of Ala-SA Molecules with C2′-*endo* (a) and C3′-*endo* (b) Ribose Puckerings, Together with the Conformation (c) Observed in the Crystalline State

The conformers of (a)—(c) correspond to entry No. 1 of C2′-*endo* and C3′-*endo* ribose puckerings and to crystal-I in Table IV, respectively.

Discussion

The solution conformation of the ala-SA molecule, studied by ^{1}H-NMR and energy calculation methods, was shown to exist as an equilibrium state among many conformations. The conformational population is solvent-dependent, especially around the glycosyl bond and exocyclic C4′–C5′ bond (Table II), implying that the molecular conformation of ala-SA is not as rigid as previously believed from X-ray crystal analysis (Tables II and IV),[12] but adapts itself well to its environment.

In D_2O solution, however, a high preference for *anti* about the glycosyl bond and *gg* orientation about the C4′–C5′ bond was observed (Table II). The *anti* orientation was also suggested from the NOE experiment. The significant NOE enhancement was observed against the H8 proton by the saturation of the H2′ proton (Table III), indicating the relatively short distance between both protons ($\chi = ca. -90°$). Concerning the orientation about the exocyclic C4′–C5′ bond, the *gg* preference of ala-SA molecule was also suggested by the torsion angle (θ) around the H–C–C–H bond, calculated from the proton vicinal coupling constants ($^3J_{vic}$, Table I) using the equation $^3J_{vic} = A\cos^2\theta - B\cos\theta + C$, where $A = 10.2$, $B = 0.8$ and $C = 0.0$.[23] Among the possible torsion angles around H4′–C4′–C5′–H5′ [$\theta = 58$ (*gg*), -117 (*gt*) or $-58°$ (*tg*)] and H4′–C4′–C5′–H5″ [$\theta = -52$ (*gg*), 52 (*gt*) or $-123°$ (*tg*)] bond sequences, the torsion angles corresponding to the *gt* or *tg* orientation deviate considerably from the standard values. Concerning the ribose puckering, a predominant population, though not extreme, of C2′-*endo* ribose puckering was suggested (Table II), and this was also supported by the empirical energy calculations, where, in general, the C2′-*endo* conformers are more stable by 2—3 kcal/mol than the C3′-*endo* conformers (Table IV).

On the other hand, as judged by the conventional NMR analysis, the conformation of the ala-SA adenosine moiety in DMSO solution could be regarded as an equilibrium state of many conformations rather than any one predominant conformation, although some conflict stems from different conformational analyses.[24]

The conformation of the L-alanylsulfamoyl moiety relative to the adenosine moiety, defined by four torsion angles β, α, ζ and ϕ, was examined by conformational energy calculations. As given in Table IV, a variety of torsion angles were observed in the energetically-stable conformers, and no notable relationship among them was found. It is important to note that the (β, ϕ) energy maps of conformers (entry No. 1—10) indicated the predominant preference of β and $\phi = ca.$ 180°, irrespective of C2′-*endo* or C3′-*endo* ribose puckering, probably as a result of the steric hindrance between the adenosine and alanylsulfamoyl moieties for β and of an electrostatic interaction between the NH_2 and O=C groups for ϕ. As a whole, the energetically-stable conformers take the folded or compact conformations in such a way that the alanyl side chain interacts side-by-side with the adenine base, irrespective of the χ and γ torsion angles and ribose puckering. It is interesting to note that although the most stable conformers belonging to respective categories [*anti-gg* (1), *syn-gg* (2), *anti-gt* (4) and *syn-gt* (6) for C2′-*endo* and *syn-tg* (1), *syn-gg* (3), *anti-gg* (6) and *anti-tg* (8) for C3′-*endo* in Table IV] showed no significant differences in energy,[25] the population of *anti-gg* with C2′-*endo* ribose puckering was predominant in conformers of < -22 kcal/mol. Thus, it appears reasonable to consider the *anti*-C2′-*endo-gg* conformation, such as the form (a) in Fig. 4, as a representative feature of ala-SA in aqueous solution.

The C2′-*endo* ribose puckering was more energetically-favorable than the C3′-*endo* one. This is in contrast to the X-ray analysis of crystalline ala-SA,[12] where two independent molecules (crystals-I and II) show a common conformation of *anti*-C3′-*endo-gt* for the adenosine moiety and *trans*(β)-*gauche*(α)-*trans*(ζ)-*trans*(ϕ) for the alanyl-sulfamoyl moiety, thus exhibiting an extended conformation (Table IV). The torsion angle γ is especially important for characterizing the whole conformation of the ala-SA molecule. Previously, we supposed that the *gt* orientation of γ was stable reflecting an intrinsic feature[12] in which the adenine base is far from the amino acid moiety, because a related tyrosyl-AMP that is bound to the cognate ARS adopts a similar open conformation.[3] However, the present study indicates that the open conformation observed for the crystal structure is in an energetically metastable state (-18.5——-19.0 kcal/mol), a relatively minor population in the solution state, and is mainly the result of the external factors such as crystal packing force.

In conclusion, the molecular conformation of ala-SA is not as rigid as expected, and is relatively flexible depending upon external factors such as solvation effects. In an aqueous solution, however, the ala-SA molecule could exhibit conformational features as shown in Fig. 4(a). Further analyses of the intrinsic conformations of other aminoacyl-SAs would help us understand how each aa-AMP is accurately recognized by its cognate ARS.

References and Notes

1) L. L. Kisselev and O. O. Favorova, *Advan. Enzymol.*, **40**, 141 (1974).
2) T. N. Bhat, D. M. Blow, P. Brick and J. Nyborg, *J. Mol. Biol.*, **158**, 699 (1982).
3) P. Brick, T. N. Bhat and D. M. Blow, *J. Mol. Biol.*, **208**, 83 (1988).
4) C. Zelwer, J. L. Risler and S. Brunie, *J. Mol. Biol.*, **155**, 63 (1982).
5) S. Brunie, C. Zelwer and J. L. Risler, *J. Mol. Biol.*, **216**, 411 (1990).
6) M. A. Rould, J. J. Perona, D. Soll and T. A. Steitz, *Science*, **246**, 1135 (1989).
7) M. Ruff, S. Krishnaswamy, M. Boeglin, A. Poterszman, A. Mitschler, A. Podjarny, B. Rees, J. C. Thierry and D. Moras, *Science*, **252**, 1682 (1991).
8) D. Vasilescu, H. Broch, R. Cornillon and J. N. Lespinasse, *J. Theor. Biol.*, **25**, 395 (1976).
9) H. Broch, R. Cornillon, J. N. Lespinasse and D. Vasilescu, *J. Theor. Biol.*, **57**, 407 (1976).
10) H. Broch, D. Vasilescu and H. Peronneau, *Studia Biophysica*, **68**, 107 (1978).
11) N. Piel, W. Freist and F. Cramer, *Bioorg. Chem.*, **12**, 18 (1983).
12) H. Ueda, Y. Shoku, N. Hayashi, J. Mitsunaga, Y. In, M. Doi, M. Inoue and T. Ishida, *Biochim. Biophys. Acta*, **1080**, 126 (1991).
13) A. V. Lakshminarayanan and V. Sasisekharan, *Biopolymers*, **8**, 475 (1969).
14) Molecular Design Ltd., CHEMLAB-II, a molecular modeling software system, San Leandro, CA, 1986.
15) M. J. D. Powell, *Comput. J.*, **7**, 155 (1964).
16) K. Akasaka, S. Shibata, T. Imoto and H. Hatano, *J. Magn. Reson.*, **17**, 413 (1975).
17) T. Imoto, K. Akasaka and H. Hatano, *Chem. Lett.*, **1974**, 73.
18) C. Chachaty, T. Zemb, G. Langlet and T. D. Son, *Eur. J. Biochem.*, **62**, 45 (1976).
19) R. Stolarski, A. Pohorille, L. Dudycz and D. Shugar, *Biochim. Biophys. Acta*, **610**, 1 (1980).
20) R. Stolarski, L. Dudycz and D. Shugar, *Eur. J. Biochem.*, **108**, 111 (1980).

21) D. B. Davies and S. S. Danyluk, *Biochemistry*, **13**, 4417 (1974).
22) D. J. Wood, F. E. Hruska and K. K. Ogilvie, *Can. J. Chem.*, **52**, 3353 (1974).
23) D. B. Davies, *Prog. NMR Spectrosc.*, **12**, 135 (1978).
24) For example, the significant NOEs between the H2′ and H8 protons (10.0%) and between the H8 and H3′ protons (5.9%) observed (Table III) suggest the existence of the *anti*-C3′-*endo* conformation about the glycosyl bond and ribose puckering, respectively, while a preference for such an *anti*-C3′-*endo* conformation is not suggested by the conventional method (Table II). Also, possible torsion angles calculated from the vicinal coupling constants [$\theta = 51°$ for H4′–C4′–C5′–H5′ and $\theta = -47°$ for H4′–C4′–C5′–H5″] indicate the *gg* preference, while equal populations of *gg* and *gt* or *tg* orientations are suggested in Table II. Such a discrepancy may reflect the coexistence of many energetically-stable conformers in DMSO solution.
25) This means that ala-SA can adopt a variety of stable conformers.